Observation of the fcc-hcp ^{4}He martensitic transformation morphology

K. A. McGreer, K. R. Lundgren, and J. P. Franck
Department of Physics, University of Alberta, Edmonton, Alberta, Canada T6G 2J1
(Received 14 February 1990)

Visual observations were made of the morphology of the fcc-hcp transformation in bulk solid helium. These visual observations provide new insight into the dynamics of the transformation on both a macroscopic and microscopic level. Observed interactions between the interface and defects in the solid provide the most direct evidence that the transformation is martensitic. Observations of the transformation occurring by the migration of a single planar interface across the entire sample provide strong evidence that the transformation is a thermoelastic martensitic transformation. This also indicates that the samples were very likely single crystals. The single planar interfaces had a preferred orientation. Some transformations occurred in which an interface rotated around a pivot. A new model of the interface structure is presented and used to explain the above results. In this model the interface consists of an array of coupled Shockley partial dislocations. The attractive interaction of the partials is described in terms of the orientation of the Burgers vectors of adjacent partials in the array.

I. INTRODUCTION

The morphology of the interfaces involved in martensitic transformations make up a large part of metallurgical investigations into martensitic transformations. Observations of the morphology often provide insight into the microscopic dynamics of the transformation. Metallurgical studies of the progress of an interface as it advances are generally restricted to studying thin foils or surface morphology. The ability to observe the interface in the bulk solid is a unique advantage to this study of solid helium. This is the first reported study (aside from a preliminary report on this work[1]) of the morphology of the martensitic transformation in bulk solid helium.

The fcc-hcp phase transformation in ^{4}He was first observed by Dugdale and Simon.[2] They attributed a specific heat anomaly to a first-order phase transition, and traced the phase line between 1.1 and 2.2 kbar. The low-temperature hcp ^{4}He phase had been identified in an earlier x-ray study by Keesom and Taconis.[3] Dugdale and Simon speculated that the high-temperature phase was the fcc phase. This was later established to be true through the x-ray diffraction studies of Mills and Schuch.[4] Theoretical predictions of the phase line by Holian *et al.*[5] stimulated interest in determining the phase line to higher pressures. Franck[6] extended the phase line to 4 kbar and Franck and Daniels[7] extended it further to 9 kbar. The transformation has been studied visually in thin films of solid helium by Franck *et al.*[8] The triple point where the fcc-hcp phase line meets the solid-fluid phase line is at 1.13 kbar and 15.0 K.[6] This means that observations of the transformation require equipment to pressurize the helium to at least 1.1 kbar and (unless a pressure much higher than 2 kbar is used) simultaneously cool the helium to about 15 K.

In a calorimetric study of the transformation, Franck[6] noted that the transformation had an athermal width and hysteresis. These kinetic factors suggested that the transformation is martensitic transformation. Franck and Daniels[7] found that consecutive fcc-hcp transformations produced hcp crystals that appeared to have their c axes in the same orientation (provided that the transformation went to completion and the fcc crystals were not allowed to anneal). The reproducibility of the c-axis orientation was direct evidence of an orientation relation between the parent and product crystals. This supported the assertion that the transformation is martensitic.

The phase line and kinetics of the fcc-hcp ^{3}He transformation[9,10] is similar to that of the fcc-hcp ^{4}He transformation.

II. THEORY

All of the models of the fcc-hcp transformation that will be considered here satisfy the Shoji-Nishiyama relation (SN relation).[11] This relation states that the close-packed plane in the hcp product (parent) crystal is parallel to one of the four close-packed planes of the fcc parent (product) crystal, and that the close-packed directions in this common plane are also parallel. A variant refers to a product crystal in a specific orientation relative to the parent crystal. An fcc crystal can produce four unique hcp variants that satisfy the SN relation. In discussing crystal planes, crystal directions, and dislocations for the fcc phase, Thompson notation[12] will be used. For the hcp phase, a similar notation based on a double tetrahedron[13] will be used. Assuming the validity of the SN relation, we adopt an additional notation convention of letting "δ plane" refer to the particular close-packed plane in the fcc parent (product) crystal that is parallel to the unique close-packed plane in the hcp product (parent) crystal (the σ plane).

None of the models considered here will involve mode softening. Ultrasonic measurements on solid ^{4}He of the

temperature dependence transverse acoustic modes as the hcp→fcc transformation was approached showed some mode softening,[14] but the softening was insufficient to be related to the mechanism of the transformation.

The fundamental agent of the fcc-hcp martensitic transformation is very likely the Shockley partial dislocation. A Shockley partial gliding on an fcc δ plane will change two close-packed planes of an fcc stacking arrangement into two close-packed planes of an hcp stacking arrangement. There are three such partial dislocations on the δ plane with Burgers vectors $\frac{1}{6}[11\bar{2}]$, $\frac{1}{6}[1\bar{2}1]$, and $\frac{1}{6}[\bar{2}11]$, these are referred to as $A\delta$, $B\delta$, and $C\delta$ in Thompson's notation. The passage of a Shockley partial on every second δ plane would cause the fcc→hcp transformation.[15] This mechanism would produce a crystal that would automatically satisfy the SN relation. Conversely, the passage of a Shockley partial on every second σ plane would cause the hcp→fcc transformation. The strongest evidence for the role of the Shockley partial as the fundamental agent of the fcc-hcp transformation comes from electron microscope observations of Shockley partials in materials in which the fcc-hcp transformation occurs. The materials observed in this way are cobalt alloys,[16–19] stainless steel,[20,21] and high-manganese steel.[22]

A transformation mechanism based on the motion of Shockley partials immediately implies that the transformation is martensitic. By definition a martensitic transformation is a solid-solid structural phase transformation that occurs by the cooperative displacement of atoms.[11,23] Here, "cooperative displacement" suggests that the displacements are correlated to some extent and occur in some kind of orderly sequence. Since a single partial glides on a single close-packed plane, the passage of a partial causes an identical displacement for each atom on that plane, i.e., the atomic displacements are correlated. A sequence for atomic displacements is also prescribed; namely, atoms directly adjacent to a partial are displaced and other atoms do not get displaced until a partial reaches them. A transformation mechanism involving motion of partial dislocations is martensitic even if it does not show features that are typical of other martensitic transformations. (Some authors prefer a more restrictive definition of "martensitic transformation"[24]).

The first model that we describe of the fcc-hcp transformation that is based on motion of Shockley partials, is the random faulting model. A single Shockley partial passing through an fcc (hcp) crystal produces a two layer structure of an hcp (fcc) stacking sequence, a stacking fault. In this model stacking faults form independently at random positions in the crystal. Gradually, the hcp (fcc) stacking sequence becomes more common in the crystal and eventually an hcp (fcc) crystal is formed. This process is similar to a second-order transformation and the order parameter is related to the fault density. Evidence for this type of transformation has been presented by Dash and Otte[25] and Fujita and Ueda.[20]

In the other two models that we describe, the transformation is more typical of a first-order transformation and has an interface separating the phases. Shockley partials lie along the interface. In the first of these two models, we consider Shockley partials having the same Burgers vector, i.e., we consider the interface to be an array of identical Shockley partials (ISPA). In this model, the square of the sum of the Burgers vectors of the partials is much larger than the sum of the squares; therefore, the energy of the array is lowest when the partials are widely separated (see the Appendix). Maximum separation may be achieved if a single partial lies on an interface at any time, a situation that may be considered an extreme case of this model. A single partial may cause an fcc-hcp transformation by traveling back and forth across its glide plane and climbing two close-packed planes at the end of each traverse.[15] Alternatively, a single partial may wind its way around a pole dislocation.[26,27] Regardless of the details, an interface with identical partials must have widely separated partials and, as a result the interface will lie close to the dislocation glide plane (the δ plane). One attraction of this model is that the plane of invariant strain under the homogeneous deformation required for the transformation (the δ plane of the fcc-hcp transformation) is close to the habit plane (the plane in which the interface lies)—a feature predicted by general theories of martensitic transformations.[28]

In addition to changing the crystal structure, the passage of this identical Shockley partial array (ISPA) through a crystal produces a shear in the crystal of 19.5° in the direction of the Burgers vectors of the Shockley partials that make up the ISPA. In a free standing crystal or a thin foil, this homogeneous strain may be accommodated by the free surfaces, but in a restrained solid this homogeneous strain must be accommodated internally in the solid. This accommodation may take place elastically (in small regions) or by slip or twinning. The amount of homogeneous strain that must be accommodated in the fcc-hcp transformation can be greatly reduced if the hcp (fcc) phase forms in alternating layers or bands in the following way: the ISPA that produces the transformation in one layer consists entirely of $A\delta$ partials, the ISPA passing through the adjacent layer consists of $B\delta$ partials, and the ISPA passing through the adjacent layer on the other side consists of $C\delta$ partials. Since the sum of the Burgers vectors is zero ($A\delta+B\delta+C\delta=0$) the average shear is zero; however, each layer will produce a local strain which must be accommodated (perhaps elastically), and therefore requires some energy for accommodation. The production of zero average strain in this way is called self-accommodation. Such bands have been observed in cobalt-nickel alloys.[29,30] The width of the observed bands were on the order of 1 μm and as small as 10–30 nm for pure cobalt.

In a second model of first-order-type transformation, we consider the interface to be an array of equal numbers of the partials $A\delta$, $B\delta$, and $C\delta$, one of which is on every second δ plane. For example, the array may consist of partials in the sequences:

$$\cdots A\delta B\delta C\delta\ A\delta B\delta C\delta\ A\delta B\delta C\delta\ A\delta B\delta C\delta \cdots .$$

We refer to such an array as a coupled Shockley partial array (CSPA). Since the square of the sum of the Burgers vectors of these partials is much less than the sum of the squares, the energy of the array is lowest when the partials are close together. (See the Appendix.) As a first ap-

proximation, we assume the partials to be sufficiently close to regard the strain fields of three neighboring partials to be centered along one line. The sum of the Burgers vectors of the partials is zero ($A\delta+B\delta+C\delta=0$), so the strain energy of any three neighboring partials is zero in this approximation. We can regard the CSPA to consist of a number of such triplets and extend the result to estimate the strain energy of the CSPA in this approximation to be zero. The only remaining energy is the core energy which is generally a small fraction of the total energy of a dislocation. In contrast, the strain energy of a partial in an ISPA remains uncanceled by its neighbors and so the energy does not approach zero and the strain energy of the individual partials remains, even when the partials are widely separated. Because of this it is reasonable to suppose that the formation of a CSPA may be energetically favorable to the formation of an ICPA. This model neglects the c-axes mismatch created when the hcp phase does not have an ideal axis ratio and neglects the volume difference between the two phases. In solid helium, the axis ratio is very close to ideal[31] and the volume change is very small,[6] so the neglect of their effects should not present a problem.

Now we consider effects of the small separation of the partials along a CPSA. We give a plausibility argument claiming that it may be energetically favorable for a CSPA to remain intact rather than separate into sections, in spite of the possibility for each section on its own to have a zero value for the sum of the Burgers vectors of the partials. Consider an array with the following sequence of partials:

$$\cdots A\delta_1 B\delta_1 C\delta_1\ A\delta_2 B\delta_2 C\delta_2 |\ A\delta_3 B\delta_3 C\delta_3\ A\delta_4 B\delta_4 C\delta_4 \cdots .$$

Subscripts have been added to the symbols for the partials to distinguish them from identical partials in other positions along the array. The section of the array left of the vertical bar has a $C\delta$ partial ($C\delta_2$) at its end. The strain field of $C\delta_2$ is reduced by the strain fields of the $A\delta_2$ and $B\delta_2$ partials and, therefore, $C\delta_2$ is bound to the left section of the array. However, since the strain fields of $A\delta_2$ and $B\delta_2$ are not centered exactly at the center of the strain field of $C\delta_2$, the cancellation of the strain field of $C\delta_2$ is not complete. Furthermore, the effectiveness of the strain fields of $A\delta_2$ and $B\delta_2$ are reduced by $C\delta_1$. For these reasons, a portion of the strain field from $C\delta_2$ remains uncanceled by the partials to the left of it. Similarly, the $A\delta_3$ and $B\delta_3$ partials will have a portion of their strain field that is not completely canceled by the strain fields of the partials to their right. The remaining portion of $C\delta_2$'s strain field can be reduced by the remaining portion of the strain field from $A\delta_3$ and $B\delta_3$ as long as they are in close proximity; therefore, the ends of the two sections will attract each other and it will be energetically favorable for the array to remain intact. The stability of the array against breaking up into sections will also likely depend on strains due to c-axis mismatch and volume differences, but this is not a problem in solid helium. The attraction of the ends of the sections is reminiscent of the attraction between electric dipoles.

Another effect of the small separation of the partials would be to produce a modulation in the elastic strain field along the array. Because most of the field is canceled, the amplitude of modulation of the field would be small compared to the strain field of a single partial. The wavelength of the modulation would be equal to three times the spacing of the partials along the array. If the array is perpendicular to the δ plane, the wavelength of the modulation would be six times the spacing of close-packed planes. This type of strain field modulation has been observed by neutron scattering in Co–32 at. % Ni during its fcc-hcp martensitic transformation.[32]

If the sections do separate, however, the sections should have a multiple of three partials in each section for the Burgers vectors of the partials in each section to sum to zero. This implies that the shortest section of a CSPA would have three coupled Shockley partials. A three partial CSPA has been observed in Co,[17] however, since the transformation in this case was strain induced, these CSPA's remained stationary while identical partials that migrated were those that could produce the strain to relax the externally applied stress.

CPSA's with other sequences of partials such as

$$\cdots A\delta_1 B\delta_1 C\delta_1\ A\delta_2 B\delta_2 C\delta_2 B\delta_3\ A\delta_3 C\delta_3 B\delta_4\ A\delta_4 \times C\delta_4 B\delta_5 C\delta_5 A\delta_5 \cdots$$

may also be possible. The $C\delta_2$ partial of this array does not have its strain field canceled by its adjacent partials; however, slightly larger sections of the array encompassing $C\delta_2$ (for example, $A\delta_2$ to $C\delta_3$) still have canceling strain fields because the Burgers vectors of the partials add to zero. We may consider the sequence given in the last paragraph to be an ideal sequence and $C\delta_2$ (and likewise $B\delta_5$) may be considered to be defects analogous to twin boundaries. An array with these defects has many more possible arrangements and may therefore occur even though its energy is likely to be higher. Arrays with even more disorder may also be possible.

The partials are coupled with a binding force because the energy of the array decreases as the partials draw nearer to each other. The binding force between the partials provides the interface with surface tension. If the attractive force between the partials dominates even at separations as small as twice the separation of close-packed planes, then the array will tend to form perpendicular to the glide plane in order to minimize the separation between the partials. Core interactions may cause repulsive forces between the partials at close proximity or noncentral forces that may favor another orientation of the array. Since the preferred habit plane (favored orientation

of the array) cannot be the δ plane (because this would widely separate the partials) and should contain one of the close-packed directions $\langle \bar{1}10 \rangle$, or AB, BC, or CA in Thompson notation (because dislocation core energies are lower in these directions), the preferred habit plane will have threefold degeneracy. For example, α, β, and γ could be the preferred habit planes, or the planes normal to $A\delta$, $B\delta$, and $C\delta$ could be the preferred habit planes. Any preferred orientation of the array may be considered in macroscopic terms as an anisotropy in the surface tension of the array.

The deformation averaged over a small region of the interface in this model is zero because the sum of the Burgers vectors of the partials is zero. This means that a transformation with a CSPA is perfectly self-accommodating and requires almost no energy to accommodate the product phase after the interface passes. (This is in contrast to the transformation mechanism with an ISPA.) Because of this, accommodation energy considerations in solids (except for thin foils and unrestrained single crystals) should favor the mechanism with a CSPA.

The cancellation of the strain fields of neighboring partials has been considered in models of nucleation embryos for the fcc-hcp transformation.[33,34] *In situ* TEM studies on a Co–32 at. % Ni single crystal give evidence of lamella growing from such nuclei,[19] and the authors of the above-mentioned neutron scattering experiment[32] interpreted their result in terms of many such embryos, each embryo being bounded by a three partial CSPA on each side. The model presented here, however, proposes a role for CSPA's beyond the nucleation stage and suggests that the coupling may lead to long coupled arrays that migrate to produce the transformation. For transformations other than the fcc-hcp transformation, however, interface models consisting of dislocation arrays have been proposed.[34]

III. EXPERIMENT

The high pressure optical cell used in this experiment was similar in design to that used by Franck and Daniels.[7] The solid helium was contained in a cylindrical region 0.48 cm in diameter and 1.3 cm in length. The ends of the cylinder were sealed with sapphire disks (0.24 cm thick) to allow for an optical path through the helium. The c axis of the sapphire windows were aligned within five minutes of arc of the optical path to minimize the optical birefringence in the sapphire. The optical aperture was restricted to 0.16 cm diameter by the rings holding the sapphire windows in place. Helium samples were solidified from isotopically pure, research grade helium (Linde ultra high purity 99.999% ^{4}He) which had less than 0.002 ppm ^{3}He. Solid helium samples are exceptionally pure because impurities precipitate out before the helium solidifies. The high-pressure capillary that filled the cell was not heated during solidification. Helium solidified in the cell at constant volume because solid helium in the capillary fill line sealed the cell. The samples were annealed after they were solidified.

The two phases of solid helium could be distinguished with polarizing optics. An fcc crystal is optically isotropic while an hcp ^{4}He crystal has uniaxial positive birefringence with the optical axis along the crystalline c axis.[35] A hcp crystal acts as an optical retardation plate with the slow axis being the projection of the crystalline c axis onto the x-y plane (the plane normal to the optical path). Light polarized along the slow axis becomes out of phase with light polarized perpendicular to the slow axis. The phase difference ϕ is given by

$$\phi = 2\pi(n_e - n_o)(d/\lambda)\sin^2\gamma \ , \tag{1}$$

where d is the thickness of the crystal, λ is the wavelength of the light, γ is the angle between the crystalline c axis and the z axis (parallel to the optical path), and $(n_e - n_o)$ is the difference between the extraordinary and ordinary indices of refraction for the effective retardation plate when the c axis is in the x-y plane. $(n_e - n_o)$ was estimated at pressures between 1 and 10 kbar by Franck and Daniels[7] and was estimated to be 7×10^{-6} for the samples used in this study. The intensity, I, of monochromatic light transmitted through a retardation plate placed between linar polarizers that make angles α and β with the slow axis is given by[36]

$$I = I_0[\cos^2(\alpha-\beta) - \sin(2\alpha)\sin(2\beta)\sin^2(\tfrac{1}{2}\phi)] \ , \tag{2}$$

The visual method for observing the transformation made use of this effect. White light from a slide projector was diffused with a diffusing screen and polarized with a linear polarizer. The polarized light was passed through the solid helium sample. The emerging light was passed through a second polarizer and then recorded with a video camera. To achieve the desired magnification, the lens of the camera was removed and replaced with a lens about 0.5 m from the camera's imaging tube. The video camera superimposed the time on the recorded image. The conductance of the thermometer was superimposed on the recorded image by using a second camera to record the digital readout of the bridge and using a video mixer to mix the images before recording the image on video tape. A time lapse recorder was used. Photographs were taken from the video monitor during play back.

Two variations of the visual method were used: the color contrast method and the intensity contrast method. The color contrast method distinguished between the two phases by the color of the light that emerged from each phase. Because the amount of retardation, ϕ, experienced by the light depends on its wavelength, λ, according to Eq. (1), white light passing through a retardation plate situated between linear polarizers emerges with a color called a "tint of passage." The tint of passage for the special cases of parallel and perpendicular polarizers are listed by Bergmann and Schaefer.[37] The color of the emerging light is most sensitive to the amount of retardation if only the light near the center of the visible spectrum is extinguished. A mica plate was inserted between the polarizers to add to the retardation produced by the hcp helium in order to help achieve the optimum amount of retardation for maximum sensitivity to change.

The intensity contrast method was done without the mica plate. With only the fcc phase present, no retarda-

tion occurs and the image was achromatic. With the hcp phase present, the retardation is small and transmitted light of all wavelengths are changed by approximately the same amount. The color of the image is washed out or unsaturated and hard to distinguish from the achromatic fcc image; however, the phases may be distinguished by the fact that the transmitted light intensity (integrated over all wavelengths) is changed for the hcp phase.

IV. RESULTS

Visual observations were made of the fcc-hcp transformation on many samples. Detailed discussion of two particular samples follow.

Sample 1 was solidified over the course of a few hours at a pressure of 1.4 kbar and annealed overnight in the fcc phase. The temperature was lowered and raised past the transition temperature (typically at a rate of 3 mK/sec) several times before the sample was melted. The kinetics of the observed transformations were typical of martensitic transformations. The average hcp→fcc transformation temperature was 14.8 K and the average fcc→hcp transformation temperature was 15.0 K. There was a hysteresis of about 0.2 K and a typical athermal width of about 20–40 mK. The color contrast method was used to record the transformation. Visual observations of eighteen transformations were made on this sample.

The optics had been adjusted in such a way that the fcc phase produced a blue image and the hcp phase produced a red image. The color of the hcp phase depends on the direction of the c axis through Eqs. (1) and (2). Since the color of the hcp image was different from the color of the fcc image, the hcp c axis was not parallel to the z axis. Furthermore, after each fcc→hcp transformation the hcp phase was indicated by nearly the same hue of red. This suggested that the hcp crystallographic orientation and crystal thickness was the same after each fcc→hcp transformation.

Figure 1 shows a sequence of photographs that illustrate one of the fcc→hcp transformations. Small dark spots present in all of the photographs of this sample were due to impurities that had precipitated onto the windows of the cell. In this sequence of images, the hcp region (red) grew and eventually replaced the fcc region. During the course of the transformation, the image was clearly divided into two distinct regions (the red and the blue regions). The boundary separating the two regions in the image was the projection of the fcc-hcp interface onto the (xy) plane. Since the boundary was very sharp, the fcc-hcp interface for this transformation was nearly parallel to the z axis. Had the interface been less parallel to the xy plane, the regions of different color in the image would have been separated by a boundary that was more graded or more diffuse. Observations indicated that the fcc-hcp interface parallel to the z axis was a plane rather than a curved surface. During the transformation the interface remained parallel to its original orientation, i.e., all sections of the interface advanced at the same rate at any given time so that the interface did not rotate. The interface migrated across the entire width of the field of view with an average velocity of 0.1 mm/sec. The interface did not advance with a constant velocity; rather, the velocity seemed to vary by a factor of 2 or more during different stages of its advance. The horizontal streaks appearing in the video images are due to an artifact of the video recorder. No event other than the parallel movement of a single planar interface was observed in this particular transformation.

Although an interface produced a sharp boundary in the observed image for over half of the transformations in this sample, six of the transformations were observed in which no sharp boundary appeared in the image. A color change with no sharp boundary in the image is what would be produced by an interface that is not sufficiently parallel to the z axis to produce a sharp boundary. In the intermediate stages of such transformations, a gradient in the color could always be seen across the image. This is what would be expected from an interface that is neither parallel to the z axis nor parallel to the x-y plane. The presence of an interface separating the fcc and hcp phases during the transformation was always demonstrated in the visual images either with the very strong evidence of a sharp boundary separating two regions of different color in the image or with somewhat weaker evidence of a gradient in the color of the image. It is very unlikely that the transformation ever occurred without an interface separating the fcc and hcp phases. The heating or cooling rate and transition temperature were the same whether the interface was parallel to the z axis or not. Six of the transformations showed only interfaces parallel to the z axis (three of which were fcc→hcp and three of which were hcp→fcc transformations) and six of the transformations showed both interfaces parallel and not parallel to the z axis in different regions of the transforming sample.

Of the six transformations that showed only interfaces parallel to the z axis, four showed nothing other than a single interface parallel to the z axis traversing the entire sample to produce the transformation. In the other two instances a second interface parallel to the z axis appeared and accounted for the transformation of a small fraction of the sample. In the cases in which both interfaces parallel and not parallel to the z axis appeared, half the cases showed two interfaces parallel to the z axis and half showed only one.

All the interfaces that were parallel to the z axis had the same orientation, i.e., their normal vectors had the same orientation in the xy plane as well as being perpendicular to the z axis. Figure 2 shows eight interfaces from different transformations in this sample that have the same interface orientation. The tendency of the interface to be in this orientation cannot be attributed to a chemical driving force because the isothermal surfaces in this sample are concentric cylinders. This shows that there was a preferred orientation for the interface, i.e., a preferred habit plane.

All but two interfaces that were parallel to the z axis first appeared at the edge of the field of view. It is reasonable to assume that the transformation started at the cell wall; i.e., it was heterogeneously nucleated. Nucleation did not occur at an embryo consisting of a rem-

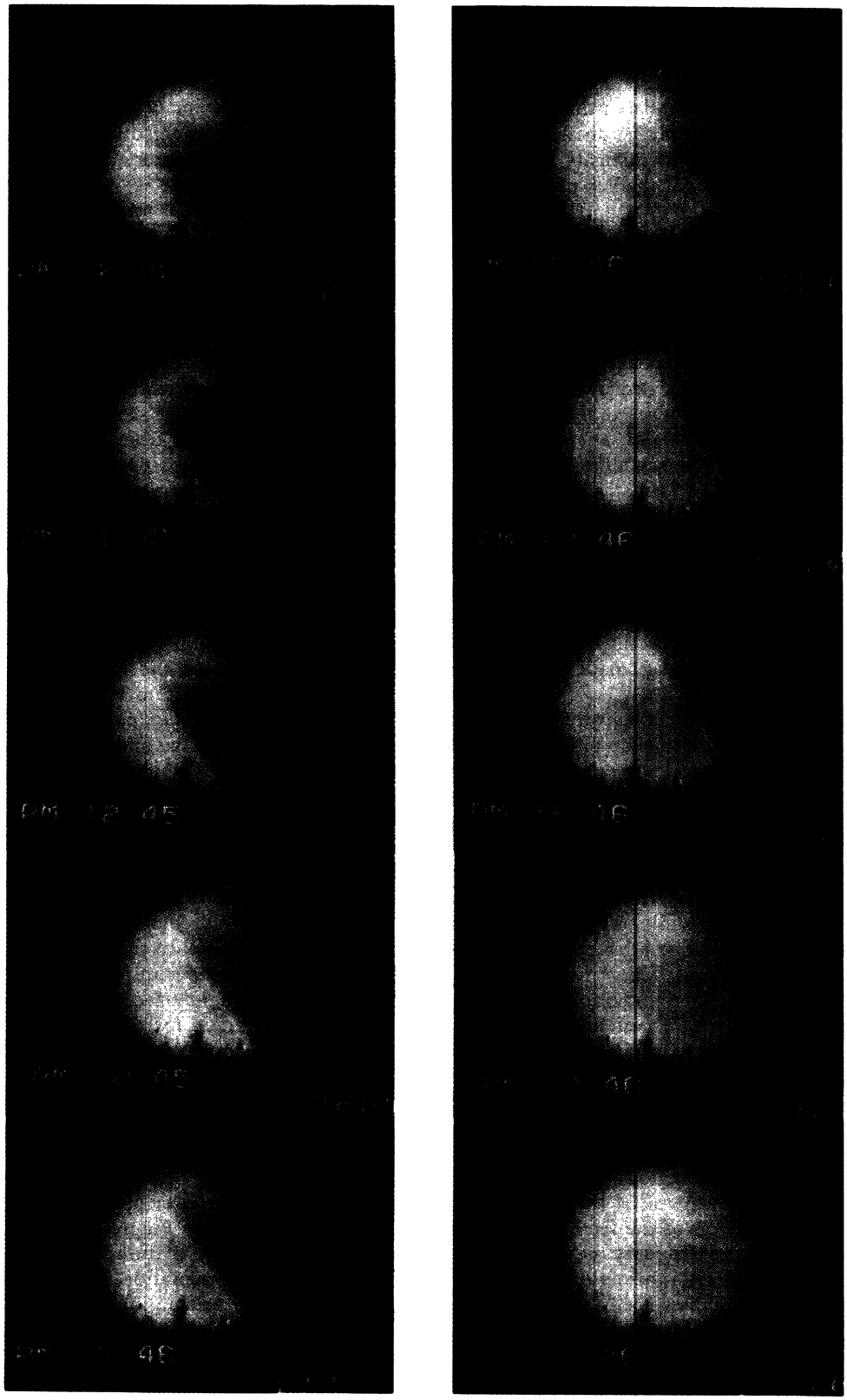

FIG. 1. One fcc→hcp ^{4}He transformation is illustrated by this sequence of images. In the first image (top left) the hcp phase forms in the lower left portion of the experimental cell. In the following images (progressing down the left column) the interface continues to advance and remain planar. The transformation continues (right column, top to bottom) until only the hcp phase is present. In these photographs the fcc ^{4}He phase appears blue, and the hcp ^{4}He phase appears red. The colors are produced as colors of (optically) thin films.

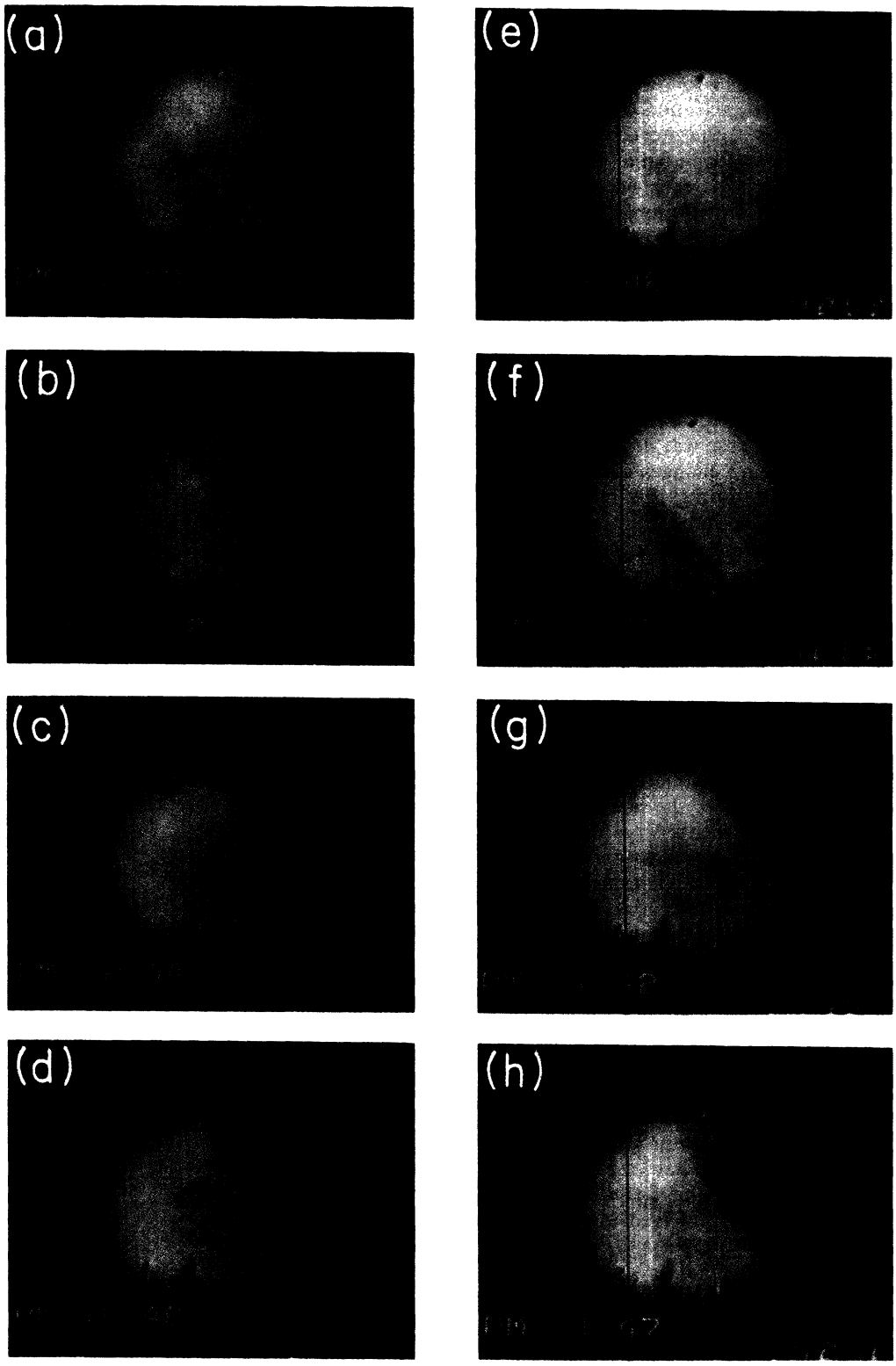

FIG. 2. Eight separate instances in which the interface had the same orientation during the fcc→hcp and hcp→fcc transformation for one ^{4}He sample. (a), (e), and (f) show the hcp→fcc (warming) transition (hcp phase in the upper right half); (b), (c), (d), (g), and (h) show the fcc→hcp (cooling) transition (hcp phase in the lower left half). The transition in each case progresses from lower left to upper right of the field of view. The reproducibility to the interface orientation supports the proposed transformation model.

nant of the parent phase of the preceding transformation. This was clear because the majority of the new phase produced in reverse transformation (the hcp→fcc following the fcc→hcp, or the fcc→hcp following the hcp→fcc) was rarely produced by the migration of an interface in the direction opposite that of the preceding transformation. In the two exceptions, a thin band, bounded by an interface parallel to the z axis on each side, gradually became apparent in the center of the sample. Although it is possible that homogeneous nucleation occurred in these cases, it is also possible that the transformation started at one of the windows in these cases. Since the majority of transformations appeared to start at the cell wall, there is visual evidence that the transformation is a heterogeneously nucleated transformation.

In one case, heating of the sample was arrested in the midst of the transformation. The interface that was parallel to the z axis in this case was held in a fixed position for three minutes and no changes whatsoever could be observed in the sample during this interval. When heating was resumed, the interface continued to advance to complete the transformation. This was a clear demonstration of the athermal character of the transformation.

Sample 2 was prepared in a very different way from sample 1. For sample 2, with an initial pressure of 1.5 kbar, solidification at constant volume was started as usual, but when the cell was about two thirds solidified, heat was applied to the sample. The heat melted the solid in the capillary, allowing more fluid to enter the cell, causing the pressure in the cell to rise to its initial pressure, 1.5 kbar. The sudden pressure increase caused rapid completion of the solidification of the sample. The result of this process was a sample with a large region of solid that had a defect density high enough to make this region opaque. This defect region was at the center of the sample and presumably ran along the z axis of the sample. The defect region, visible in all of the photographs of this sample, was in the shape of a crescent opening downwards and an additional small very dark spot just below the crescent. The intensity contrast method was used for this sample.

Many of the observations on this sample were similar to those on sample 1. Several observations were made of single planar interfaces oriented parallel to the z axis migrating across the entire sample to produce the transformation. This sample appeared to have a preferred orientation that was different from the preferred orientation in sample 1. The fact that the preferred orientation was different in a different sample supports the interpretation that the preferred interface orientation was relative to the crystal orientation and not an artifact of the walls of the cell. Several transformations were observed in which the interface was not parallel to the z axis.

The defect region in this sample produced effects that were not seen in sample 1. In many transformations, the progress of an interface appeared to be hindered by the defect region. An example of such a transformation is illustrated in Fig. 3. The column on the left shows photographs of the transformation and the column on the right contains drawings that were traced from the photographs to highlight the features of interest. The photographs only faintly show the interface; however, the moving image from the video tape clearly shows the motion of the interface and was used as a guide to tracing the interface from the photographs. The defect region appeared to interrupt the motion of the interface where the two intersected and yet did not stop the rest of the interface from advancing. Figure 3 illustrates an interface to the left of the defect region that was advancing in one section and trailing in another section. The advancing section remained planar and in the preferred orientation, while the other section trailed off to remain connected to the stationary defect region. The advancing section of the interface is connected to the trailing section with a rounded corner rather than a sharp corner.

In other transformations in this sample, an interface remained fairly planar and progressed by rotating about a pivot that was located at the defect region. In some cases, the fcc phase formed into a wedge shape with the defect at the point of the wedge and the wedge extending to the cell wall. In these cases, the hcp→fcc transformation progressed by both interfaces pivoting about the line of the defect to make the wedge wider. When the transformation was reversed before it was allowed to go to completion, the fcc→hcp transformation progressed by both interfaces rotating to shrink the wedge. These transformations appeared so faintly on the video image that the interfaces could not be seen on the monitor once the video was held in freeze frame.

Some observations were made of the transformation occurring in this sample by the passage of curved interfaces. These interfaces sometimes changed their shape as

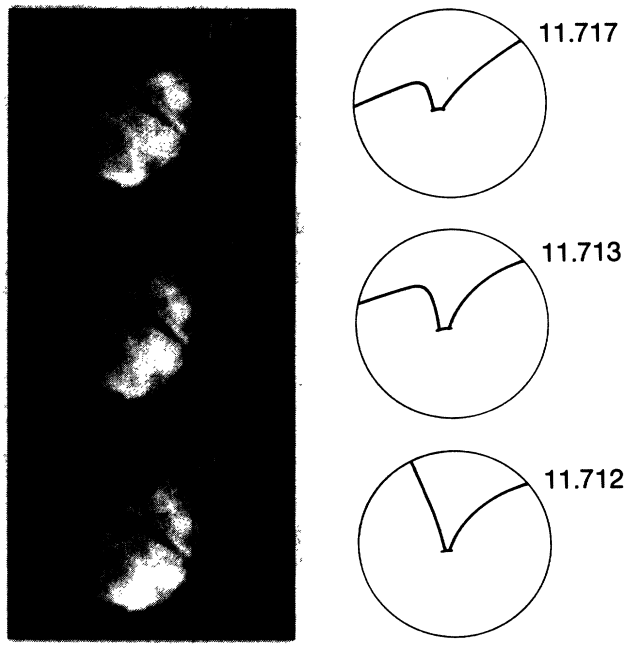

FIG. 3. A defect at the center of the solid was observed to effect the progress of the interface during the fcc→hcp transformation. The sketches in the right column highlight the interface in the images in the left column as the transformation progresses (top to bottom).

the transformation progressed. These transformations appeared so faintly on the video image that they could not be seen on the monitor once the video was held in freeze frame.

Very rapid cooling sometimes produced results very different from the results observed with slow cooling. When sample 2 was cooled at 60 mK/sec to 14.50 K, parallel bands of light and dark regions began to appear. Figure 4 shows images of the sample in various stages of the formation and disappearance of these bands. Evidence of the fcc→hcp transformation in a portion of the sample was observed at 14.6 K. Both bands that were lighter and bands that were darker than the original shade of grey, appeared in the image. A light band and a dark band usually appeared simultaneously. Each band first appeared as a faint band and, with time, became wider and more distinct. The distinctiveness and number of the bands increased until the temperature reached 14.39 K. Below 14.39 K, the bands began to fade away and at 14.34 K there was very little trace of the bands. As the bands faded, most appeared to fade on the right side of the image before they faded on the left. It appeared that the bands faded away by reducing their length rather than their width. It is noteworthy that these bands were aligned parallel to the preferred interface orientation in this sample.

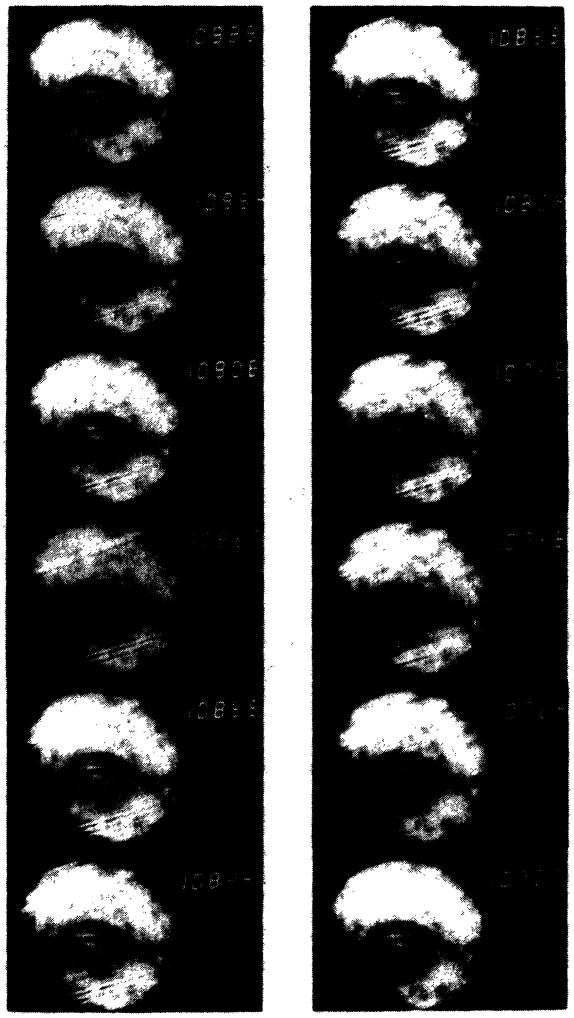

FIG. 4. Sequence of images showing parallel bands that formed (left column) and subsequently faded (right column) during rapid cooling through the fcc→hcp transformation.

Many other samples of solid helium were studied. It appeared that the crystal orientation in the cell was random and since we could not rotate the sample, interfaces happening to be parallel to the z axis rarely occurred, as one would expect. The unfortunate result of this is that few observations were as illustrative as the ones presented here. For most observations the interface was not parallel to the z axis. In some observations, the hcp c axis was oriented such that there was very little contrast between the hcp and fcc phases.

V. DISCUSSION

Because it appeared that an interface always separated the fcc and hcp phases during the transformation, the transformation did not occur by the random faulting process described in the first model mentioned in Sec. II. Since the migration of the one interface was sufficient to transform the sample, there are no intermediate phases in the fcc→hcp or hcp→fcc transformations.

Generally, grain boundaries interrupt the progress of the interface in a martensitic transformation. The migration of an interface across the entire width of sample 1 indicated that no grain boundaries were in the path of the interface. If the interface extended the entire length of the sample (from the front window to the back window), as appeared to be the case, the interface swept through the entire sample without encountering a grain boundary; i.e., the sample was a single crystal. In sample 2, transformations occurred in which one interface traversed the entire width of the sample and yet other interfaces were observed during the same transformation. It is likely that sample 2 had large grains (one of which spanned the field of view) but was not a single crystal. The production of a large grain sample in spite of a pressure pulse being applied to the sample is consistent with the observations on solid helium by Mills and Schuch.[38]

Transformations occurring by the passage of a single interface across the entire sample, as observed in sample 1, are uncommon in martensitic transformations. Usually, strains associated with the transformation process accumulate until they cause sufficient plastic deformation to destroy the interface coherency conditions that are necessary for the progress of the interface. This usually occurs before the interface reaches a grain boundary. The exceptions [Au-Cd (Ref. 39), In-Th (Refs. 40 and 41), Cu-Al-Ni (Ref. 42) alloys], i.e., the martensitic transformations that occur by the migration of a single interface across the sample, are thermoelastic martensitic transformations and have small shape strain associated with the transformation. The essential feature of a thermoelastic martensitic (TEM) transformation is that it has a mobile interface (for both directions of the transformation) and low driving force for the transformation.[11,43] (This definition appears to be fairly well accepted in spite of

notable objections[44] and its difference from the original usage.[45]) It is recognized that materials that frequently had mobile interfaces during transformation did not always have mobile interfaces; low cooling rates, interruption of the progress of the interface, or disruption of the self-accommodation process could immobilize the interface (i.e., stabilization could occur). Nevertheless, these materials were considered to be TEM materials. The migration of an interface across the entire crystal in solid helium indicates that the transformation is a thermoelastic martensitic transformation.

We now compare the results from sample 1 with the prediction of the ISPA model that the interface should lie near the δ plane. Observations of the reproducibility of the color of the image of the hcp phase, indicating that the c axis was reproduced in the same orientation every time the hcp phase appeared, implied that the δ plane orientation was also reproduced. Since the plane of the interface appeared in orientations both parallel and not parallel to the z axis, and yet the δ plane was always in the same orientation, the interface had to be along a plane different from the δ plane at least some of the time. In this respect the ISPA model is not consistent with the observations on sample 1.

The CSPA model, on the other hand, allows for three preferred interface orientations. One of the preferred interface orientations could have been the orientation parallel to the z axis that was observed. The other two orientations could account for the observed interfaces that were not parallel to the z axis. The interface could have been consistently migrating in any of these preferred orientations and produce the hcp c axis in the same orientation. In this respect the CSPA model is consistent with the observations in sample 1.

The fact that the hcp phase was produced in the same orientation each time it was produced in sample 1, when four variants of different orientations were consistent with the SN relations, suggests that there was a preference for a particular variant to be produced in the fcc$\rightarrow$hcp transformation. It may be that, due to stacking faults in the crystal, one of the fcc close-packed planes is an easier glide plane for dislocations and, since the glide plane is the δ plane in the CSPA model (using our convention of labeling the plane parallel to the σ plane as the δ plane), determining the glide plane determines which hcp variant will be produced. The determination of which variant grows may be sensitive to many details. An interesting illustration of this sensitivity is the fcc-hcp martensitic transformation in solid hydrogen. In H_2, the same hcp variant is reproduced in a sequence of transformations, but in D_2, this does not occur.[46,47]

The reproducibility of the hcp orientation in a sequence of transformations and the existence of a preferred interface orientation (both of which are features that are associated with martensitic transformations[43] add to existing evidence that the transformation is martensitic. The observation that crystal defects interfered with the progress of the transformation in sample 2 was the most direct evidence that the transformation was martensitic. If the atomic displacements are to be highly correlated, the advance of the interface requires atoms to move from specific lattice sites of the parent crystal to specific sites of the product crystal. Defects in the parent crystal will result in atoms not being at the sites on which the transformation mechanism was "designed" to operate. Civilian transformations, by contrast, do not have highly correlated atomic displacements and therefore do not require the atoms in the parent crystal to be at specific sites, i.e., lattice defects should not severely hinder civilian transformations.

The observation illustrated in Fig. 3 can be explained in terms of the CSPA model. The defect region may have blocked the migration of the partials that were traveling on glide planes that intersected the defect region. The section of the interface containing partials gliding on unblocked glide planes would have continued to advance and remain in the preferred orientation. The blocked glide planes would remain untransformed in the "shadowed" side of the defect region. This could happen so long as the surface tension in the interface was low enough to permit the corner formed between the advancing section of the interface and the trailing section of the interface that extended back to the defect region.

An interface that appeared to rotate about a pivot was also frequently observed. In the ISPA model, the interface must remain parallel to the δ plane and, therefore, cannot rotate. In the CSPA model, the interface tends to lie in the preferred orientation because of second-order energy considerations; however, if the interface is prevented from advancing in this orientation, the chemical driving force behind the transformation may be sufficient to force the interface out of its preferred orientation. Outside of the preferred orientation, the interface may be kept roughly planar by the surface tension in the interface. If the interface is kept roughly planar and pinned along one line, it can only advance by rotating about that line.

Light and dark bands sometimes appeared during rapid cooling or heating. Since both bands (those lighter and those darker than the original shade of grey) formed, at least two variants formed that did not have the fcc structure. Both of these variants may have been the hcp phase, or one or both may have been a metastable close-packed phase. These bands may have formed during twinning or during the structural phase transformation. Although the cause of the bands is not clear, the formation of the bands does not appear inconsistent with the CSPA model.

VI. SUMMARY

Observations that the transformation was affected by crystal defects in the solid provide the most direct evidence that the fcc-hcp transformation in ^{4}He is a martensitic transformation. The transformation exhibited hysteresis and athermal transformation kinetics. The hcp crystal orientation was reproduced in consecutive transformations. The interface had a preferred orientation. The transformation sometimes occurred by the migration of a single planar interface across the entire sample. This indicated that the transformation is self-accommodating and is the strongest evidence that the transformation is a

thermoelastic martensitic transformation. An extraordinary observation was made of a transformation that occurred as an interface rotating about a pivot. The pivot was at the site of a defect region in the crystal to which the interface was pinned. The fact that the interface could rotate can be accounted for if the interface is modeled by an array of coupled Shockley partial dislocations. The partials in the coupled Shockley partial array (CSPA) can be attracted to each other if the Burgers vectors of adjacent partials sum to zero. This model can also explain other observed interactions between the interface and defects in the solid as well as details of the preferred interface orientation. The observations are not consistent with interface models presently in the literature, but are consistent with the new model (the CSPA model) presented here.

ACKNOWLEDGMENTS

This research was supported in part by grants from the National Sciences and Engineering Research Council of Canada.

APPENDIX

Most of the energy of a single isolated dislocation with Burgers vector b_n is the elastic strain energy U_n, which can be approximated as[48]

$$U_n = A|b_n|^2 , \tag{A1}$$

where A is given by

$$A = \frac{GL \ln(R/r_0)}{4\pi(1-\nu)}(1-\nu\cos^2\alpha) , \tag{A2}$$

where G is the shear modulus, L is the dislocation length, ν is the Poisson ratio, R and r_0 are the outer and inner radii of the cylindrical region over which the elastic approximation for the strain field is valid, and α is the angle between the dislocation line and the Burgers vector. R may be taken to be the radius of the grain and r_0 may be taken to be on the order of $|b_n|$. Careful estimation of R and r_0 is not necessary because U is not sensitive to their values. Since ν is about $\frac{1}{3}$, the value of $(1-\nu\cos^2\alpha)$ will vary by less than a factor of 2. Therefore, within a factor of 2, A is independent of the Burgers vector b_n.

The energy of an assembly of dislocations that are so widely separated that their elastic strain fields do not interact significantly is given by

$$U = \sum_n U_n = A \sum_n |b_n|^2 . \tag{A3}$$

At the other extreme, the separation between the dislocations in an assembly may be so small the strain field of each dislocation may be approximately centered on the same line. The effective Burgers vector is the sum of the Burgers vectors of dislocations in close proximity $\sum_n b_n$ and the energy of the group can be approximated as

$$U = A \left| \left[\sum_n b_n \right] \right|^2 . \tag{A4}$$

In short, an assembly of widely separated dislocations has an energy approximately proportional to the sum of the squares of the Burgers vectors, and an assembly of dislocations in close proximity has an energy approximately proportional to the square of the sum of the Burgers vectors.

[1]J. P. Franck and K. A. McGreer, in *Proceedings of the International Conference on Martensitic Transformations,* Nara, 1986, edited by I. Tamura (Jpn. Inst. Metals, Aoba Aramaki, Sendai, 1987), p. 1104; J. P. Franck, K. R. Lundgren, and K. A. McGreer, Physica B **140**, 230 (1986).
[2]J. S. Dugdale and F. E. Simon, Proc. R. Soc. London Ser. A **218**, 291 (1953).
[3]W. H. Keesom and K. W. Taconis, Physica **5**, 161 (1938).
[4]R. L. Mills and A. F. Schuch, Phys. Rev. Lett. **6**, 263 (1961).
[5]B. L. Holian, W. D. Gwinn, A. C. Luntz, and B. J. Alder, J. Chem. Phys. **59**, 5444 (1973).
[6]J. P. Franck, Phys. Rev. B **22**, 4315 (1980).
[7]J. P. Franck and W. B. Daniels, Phys. Rev. B **24**, 2456 (1981).
[8]J. P. Franck, J. Gleeson, K. E. Kornelsen, J. R. Manuel, and K. A. McGreer, J. Low Temp. Phys. **58**, 153 (1985).
[9]J. P. Franck, Phys. Rev. Lett. **7**, 435 (1961).
[10]M. G. Ryschkewitch, J. P. Franck, B. J. Duch, and W. B. Daniels, Phys. Rev. B **26**, 5276 (1982).
[11]Z. Nishiyama, *Martensitic Transformations* (Academic, New York, 1978).
[12]N. Thompson, Proc. Phys. Soc. London, Sect. B **66**, 481 (1953).
[13]A. Berghezan, A. Fourdeux, and S. Amelinckx, Acta Metall. **9**, 464 (1961).
[14]K. A. McGreer and J. P. Franck, Jpn. J. Appl. Phys. Suppl. **26-3**, 409 (1987); Phys. Rev. B **41**, 162 (1990).
[15]J. W. Christian, Proc. R. Soc. London, Sect. A **206**, 51 (1951).
[16]E. Voltava, Acta Metall. **8**, 901 (1960).
[17]S. Mahajan, M. L. Green, and D. Brasen, Metall. Trans. A **8**, 283 (1977).
[18]I-Wei Chen and Y-H Chiao, Acta Metall. **33**, 1827 (1985).
[19]C. Hitzenberger, H. P. Karntaler, and A. Korner, Acta Metall. **36**, 2719 (1988).
[20]H. Fujita and S. Ueda, Acta Metall. **20**, 759 (1972).
[21]J. A. Venables, Philos. Mag. **7**, 35 (1962); Z. Nishiyama, Metal Physics **7**, 107 (1961).
[22]H. Schumann, Arch. Eisenhütt. **38**, 647 (1967); **40**, 1027 (1969).
[23]C. M. Wayman, in *Encyclopedia of Materials Science and Engineering,* edited by M. B. Bever (MIT Press, Cambridge, Massachusetts, 1986), p. 2736.
[24]M. Cohen, G. B. Olson, and P. C. Clapp, *Proceedings of the International Conference on Martensitic Transformations, ICOMAT 1979 Cambridge, Mass.* (Department of Materials Science and Engineering, Massaschusetts Institute of Technology, Cambridge, Mass., 1979); W. S. Owen, in *Encyclopedia of Materials Science and Engineering* (Ref. 23), p. 2736; J. W. Christian, *ibid.*, p. 3496.
[25]J. Dash and H. M. Otte, Acta Metall. **11**, 1169 (1963).
[26]Z. Seeger, Metallk. **44**, 247 (1953).

[27]Z. S. Basinski and J. W. Christian, Philos. Mag. **44**, 791 (1953).
[28]J. W. Christian, *The Theory of Transformations in Metals and Alloys* (Pergamon, New York, 1965).
[29]S. Takeuchi and T. Honma, Sci. Rep. Res. Inst. Tohoku Univ. **9A**, 492 (1957).
[30]H. Bibring, F. Sebilleau, and C. Buckle, J. Inst. Metall. **87**, 71 (1958-1959).
[31]J. P. Franck and R. Wanner, Phys. Rev. Lett. **25**, 345 (1970), and references therein.
[32]O. Blachko, G. Krexner, J. Pleschiutchnig, G. Ernst, C. Hitzenberger, H. P. Karnthaler, and A. Korner, Phys. Rev. Lett. **60**, 2800 (1988).
[33]G. B. Olson and M. Cohen, Metall. Trans. **7A**, 1897 (1976).
[34]G. B. Olson and M. Cohen, Metall. Trans. **7A**, 1905 (1976).
[35]J. E. Vos, R. V. Kingma, F. J. van der Gaag, and B. S. Blaisse, Phys. Lett. **24A**, 738 (1967).
[36]R. S. Longhurst, *Geometric and Physical Optics* (Longman, London, 1973).
[37]L. Bergmann and C. Schaefer, *Optik* (Walter de Gruyter, Berlin, 1966).
[38]R. L. Mills and A. F. Schuch, J. Low Temp. Phys. **16**, 305 (1974).
[39]L. C. Chang and T. A. Read, Trans. Am. Inst. Min. Metall. Eng. **191**, 47 (1951).
[40]M. W. Burkart and T. A. Read, Trans. Am. Inst. Min. Metall. Eng. **196**, 1516 (1953).
[41]Z. S. Basinski and J. W. Christian, Acta Metall. **2**, 148 (1954).
[42]K. Otsuka, M. Takahashi, and K. Shimizu, Metall. Trans. **4**, 2003 (1973).
[43]C. M. Wayman, in *Martensitic Transformations: An Overview Proceedings of the International Conference on Solid→Solid Phase Transformations,* edited by H. I. Aaronson, D. E. Laughlin, R. F. Sekerka, and C. M. Wayman (The Metallurgical Society of AIME, Warrendale, PA, 1981), p. 1119.
[44]G. B. Olson and M. Cohen, Scr. Metall. **10**, 359 (1976).
[45]G. V. Kurdjumov and L. G. Khandros, Dokl. Acad. Nauk USSR **66**, 211 (1949).
[46]R. Banke, M. Calkins, and H. Meyer, J. Low Temp. Phys. **61**, 193 (1985).
[47]R. Banke, X. Li, and H. Meyer, Phys. Rev. B **37**, 7337 (1988).
[48]D. Kuhlmann-Wilsdorf, in *Physical Metallurgy,* edited by R. W. Cahn (Wiley, New York, 1965).

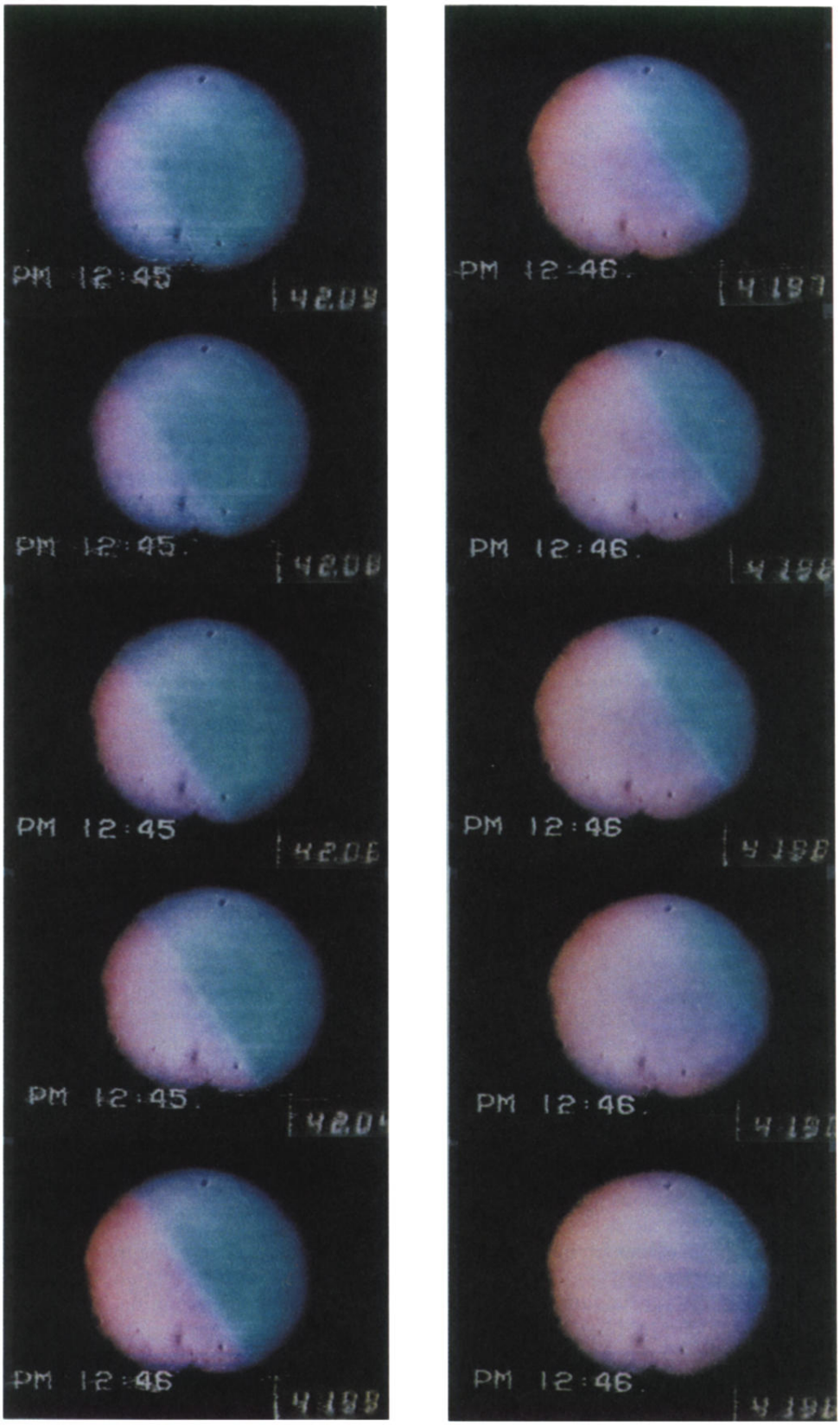

FIG. 1. One fcc→hcp ^{4}He transformation is illustrated by this sequence of images. In the first image (top left) the hcp phase forms in the lower left portion of the experimental cell. In the following images (progressing down the left column) the interface continues to advance and remain planar. The transformation continues (right column, top to bottom) until only the hcp phase is present. In these photographs the fcc ^{4}He phase appears blue, and the hcp ^{4}He phase appears red. The colors are produced as colors of (optically) thin films.

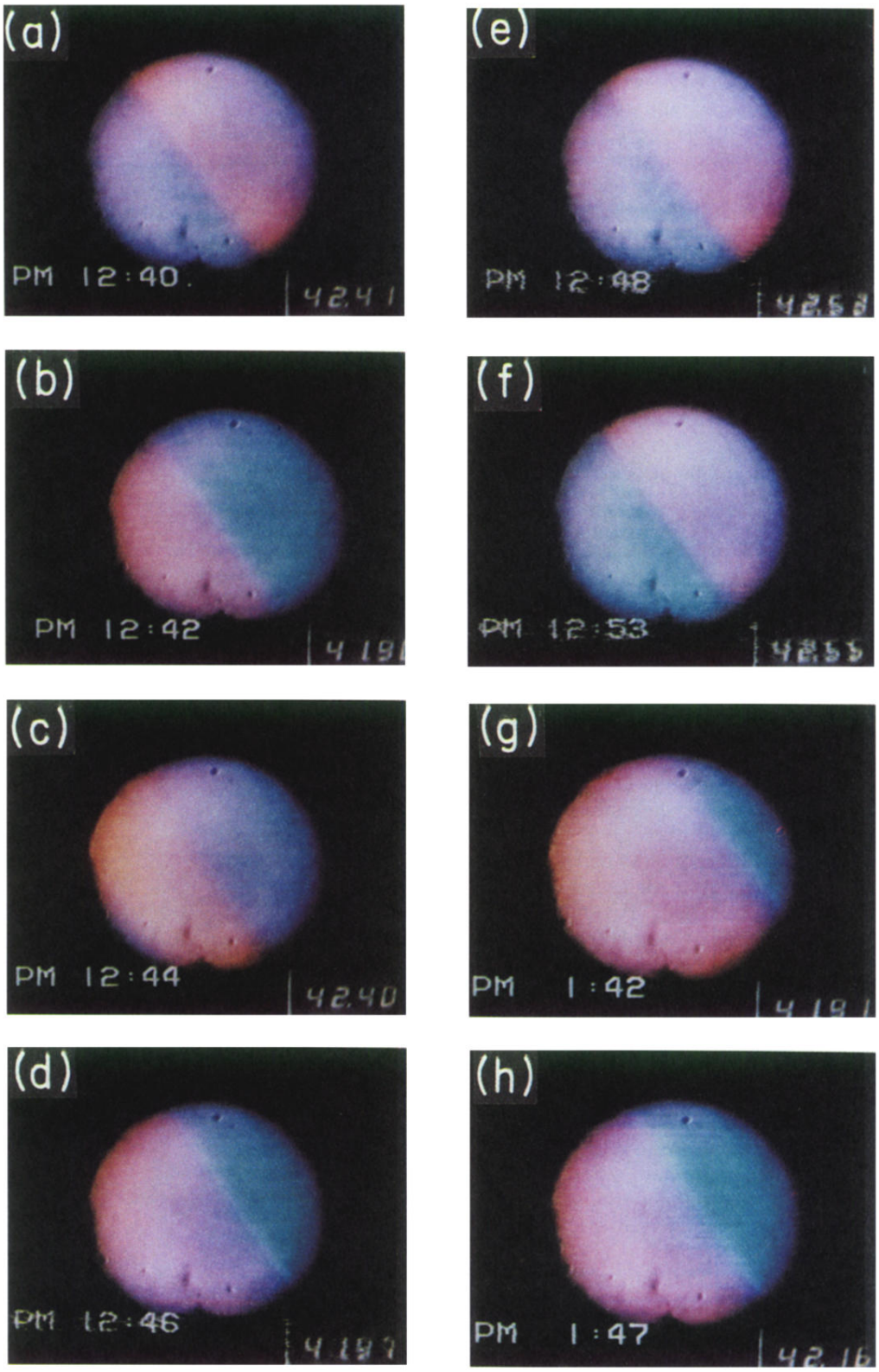

FIG. 2. Eight separate instances in which the interface had the same orientation during the fcc→hcp and hcp→fcc transformation for one ^{4}He sample. (a), (e), and (f) show the hcp→fcc (warming) transition (hcp phase in the upper right half); (b), (c), (d), (g), and (h) show the fcc→hcp (cooling) transition (hcp phase in the lower left half). The transition in each case progresses from lower left to upper right of the field of view. The reproducibility to the interface orientation supports the proposed transformation model.

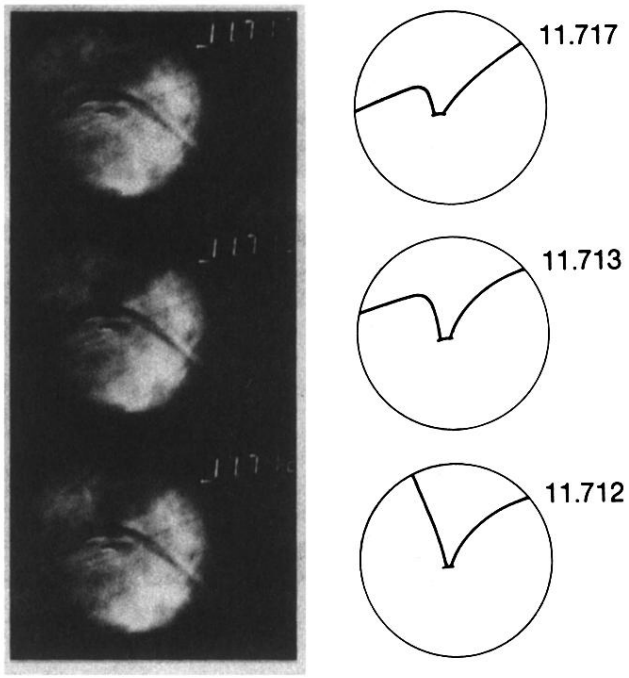

FIG. 3. A defect at the center of the solid was observed to effect the progress of the interface during the fcc→hcp transformation. The sketches in the right column highlight the interface in the images in the left column as the transformation progresses (top to bottom).

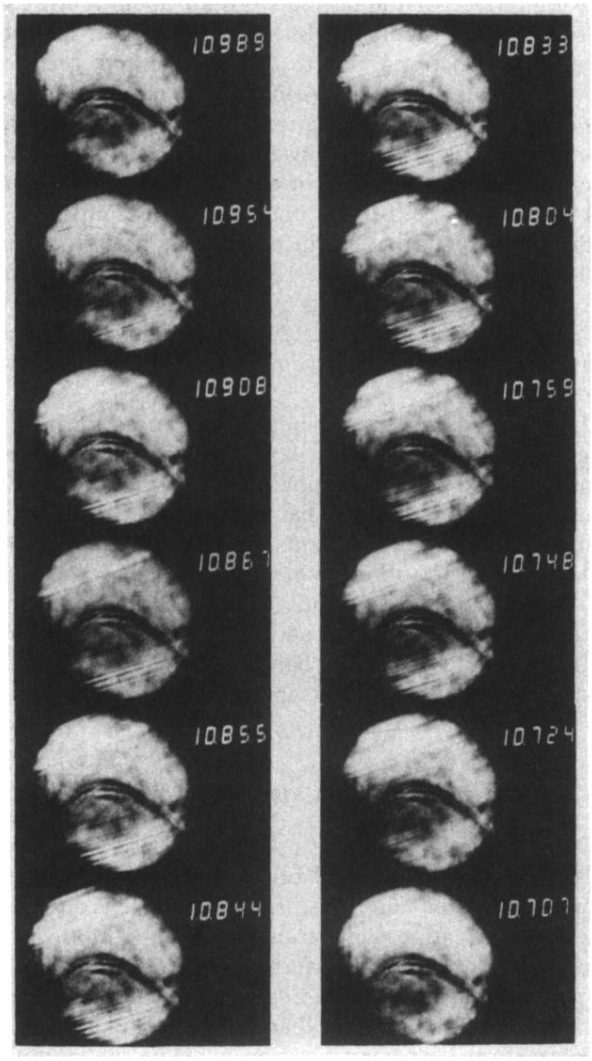

FIG. 4. Sequence of images showing parallel bands that formed (left column) and subsequently faded (right column) during rapid cooling through the fcc→hcp transformation.